ELSEVIER

International Journal of Mass Spectrometry 182/183 (1999) 381–402

International Journal of Mass Spectrometry

Isotope effects in dissociation reactions of proton bound amine dimers in the gas phase

K. Norrman[a], T.B. McMahon[b,*]

[a]*Department of Chemistry, University of Copenhagen, Copenhagen, DK-2100 Copenhagen Ø, Denmark*
[b]*Department of Chemistry, University of Waterloo, Waterloo, Ontario N2L 3G1, Canada*

Received 3 August 1998; accepted 4 November 1998

Abstract

Kinetic and thermodynamic isotope effects on the unimolecular dissociation of proton bound dimers were studied in the gas phase using mass spectrometry techniques. In addition proton transfer reactions were investigated using equilibrium techniques in conjunction with a theoretical study. Normal isotope effects were observed for all of the amine systems studied. The effect of label position, extent of labeling, size and structure of the proton bound dimers have been discussed with respect to (i) the kinetic and thermodynamic isotope effect on the dissociation reaction, (ii) the kinetic energy release on the dissociation reaction, (iii) the thermodynamic isotope effect on the proton exchange reaction between the labeled and unlabeled amines, and (iv) the effective temperatures and the excess energies of the metastable proton bound dimers. Other compound classes (CH_3OH, $(CH_3)_2O$, CH_3CN and $(CH_3)_2CO$) were studied and discussed in the same way, though not as thoroughly. All the systems show normal isotope effects, except for the proton bound dimer of CH_3CN and CD_3CN, which showed an inverse isotope effect. (Int J Mass Spectrom 182/183 (1999) 381–402) © 1999 Elsevier Science B.V.

Keywords: Deuterium isotope effects; Proton bound dimers; Kinetic method; Proton affinity; Effective temperature; Deuterium labeled amines; Kinetic energy release

1. Introduction

Isotope effects on gas phase reactions have been studied extensively in the past [1–3]. The main reason to study isotope effects is to obtain information about structure and reaction mechanisms. Many such studies have dealt with observations of primary hydrogen isotope effects, often with the implicit assumption that any secondary isotope effects will be small, which may not always be a reasonable premise. The literature contains many examples of secondary isotope effects on ionic reactions, in most cases related to compounds that contain only covalent bonds [1–24]. For compounds with hydrogen bonds (e.g. proton bound dimers) only a few examples have been reported [25–28].

Isotope labeling affects reaction rates, in many cases by a combination of primary and secondary isotope effects. Often it is difficult quantitatively as well as qualitatively to distinguish between the two contributions without a systematic study of the secondary isotope effects.

For competing reactions (e.g. Eq. (1)) intramolecular secondary isotope effects arise when there is a

* Corresponding author.

Dedicated to the memory of Ben Freiser who was a great friend as well as a great scientist.

PII S1387-3806(98)14259-8

difference between the number of quantum states in the two transition states (TS), Eq. (2) [29,30].

$$CH_3NH_3^+ + CD_3NH_2 \overset{k_D}{\leftarrow} \underset{\mathbf{1}}{(CH_3NH_2)(CD_3NH_2)H^+} \overset{k_H}{\rightarrow} CH_3NH_2 + CD_3NH_3^+ \quad (1)$$

$$k_H/k_D = \frac{G^{\#}(E - E_{0,H})}{G^{\#}(E - E_{0,D})} \quad (2)$$

k_H/k_D is the kinetic isotope effect, $G^{\#}$ the state sum, E is the internal energy and E_0 the critical energy. For normal secondary isotope effects ($k_H/k_D > 1$) the critical energy is lower for loss of CH_3NH_2 from **1** than for loss of CD_3NH_2 as a result of the influence of isotopic substitution on the zero-point energies (ZPE) of the two transition states. The C–H(D) vibrational frequencies are lowered in the TS. The absolute change is larger when the C–H frequencies are involved. The effect of the ZPE difference on the relative rates is particularly pronounced when the internal energy is low. The secondary isotope effect on the dissociation of the proton bound dimer, thus, increases with ion lifetime.

The thermodynamic isotope effect is manifested in the reaction enthalpy and, thus, in the equilibrium constant, K_{eq}. For a normal isotope effect $K_{eq} < 1$, which corresponds to Eq. (3) being endoergic, that is favoring the protonation of the labeled amine.

$$CD_3NH_3^+ + CH_3NH_2 \overset{K_{eq}}{\rightleftarrows} CD_3NH_2 + CH_3NH_3^+ \quad (3)$$

Secondary isotope effects on gas phase reactions of ions can be investigated using a mass spectrometer. For simplicity, it is desirable to study systems that do not show other competing reactions. In a mass analyzed ion kinetic energy spectrometry (MIKES) experiment [31] the relative ion yields will, because of the narrow time window for the reactions of metastable ions, be a measure of the isotope effect [1].

The kinetic method (Cooks' method) [32–34] can be used to study the effect of isotopic labeling on proton affinities (PA). The collision induced or spontaneous dissociation, e.g. Eq. (1), of a proton bound dimer results in formation of both monomers. In the absence of entropy effects and assuming that the activation energies for the reverse reactions are negligible, the product ion intensity ratio will reflect the difference in proton affinity between the two bases. Proton bound dimers of isotopomers are ideal systems for application of the method, because many of the errors that limit the kinetic method, are avoided, because of the similarity of the two monomers involved. From the isotope effect it is, thus, possible to derive thermochemical information, Eq. (4).

$$\ln (k_H/k_D) \approx \ln (I_H/I_D) \approx \Delta PA/RT_{eff} \quad (4)$$

I_H is the intensity of the product ion BH^+-d_n, I_D is the intensity of the product ion BH^+, ΔPA is the difference in proton affinity between B and B-d_n, R is the gas constant and T_{eff} is the so-called effective temperature [35] of the metastable parent ion (the proton bound dimer).

Nourse and Cooks [25] used an ion trap mass spectrometer to study the influence of deuterium substitution on the reactions of 2-pentanone and acetophenone and demonstrated that the kinetic method reliably detects very small proton affinity differences. As a reference they investigated *paradeuterium* labeled benzoic acid and *metadeuterium* labeled benzoic acid relative to unlabeled benzoic acid. These systems are not expected to show any secondary isotope effects, since they are labeled remote from the dominant protonation site. For the *parasystem* they measured a relative ion yield (I_H/I_D) of 0.9 ± 0.1, and for the *metasystem* they obtained 1.0 ± 0.1. Because they could not detect any isotope effect, they concluded that the method is well suited for measuring small proton affinity differences. For the $CH_3COCD_2CH_2CH_3$ system they observed an inverse secondary isotope effect of 0.48, which they took to correspond to a ΔPA of 0.16 ± 0.08 kcal/mol (the nondeuterium labeled ketone having the higher proton

affinity). For the $PhCOCD_3$ system they observed a normal secondary isotope effect of 1.4, which they took to correspond to a ΔPA of 0.07 ± 0.07 kcal/mol (the deuterium labeled ketone having the higher proton affinity).

Dang et al. [27] used tandem flowing afterglow-selected ion flow tube mass spectrometry with collision induced dissociation (CID), to study the effect of deuterium substitution on the dissociation of proton bound dimers of ethoxide. They found that deuterium substitution increases the proton affinity of the ethoxide (normal isotope effect). $PA(CH_3CD_2O^-)$ is increased by 0.34 ± 0.15 kcal/mol relative to $PA(CH_3CH_2O^-)$, $PA(CD_3CH_2O^-)$ by 0.18 ± 0.15 kcal/mol and $PA(CD_3CD_2O^-)$ by 0.48 ± 0.15 kcal/mol. Ab initio calculations of the zero-point energy differences at the HF/6-311++G(d,p) level gave practically the same values. Their results suggest that deuterium labeling in the α position has a greater effect on the proton affinity than in the β position, consistent with their relative distances from the protonation site. Furthermore the effect seems to increase with an increasing number of deuterium substitutions, which is a rational observation. Related studies describe the influence of deuterium substitution on proton bound dimers of hydroxide, [36] methoxide [26,37–39] and isopropoxide [40].

Haas and Harrison [26] examined the CID of proton bound ethoxide and methoxide dimers. They found that the proton affinity increases 0.6 kcal/mol for CD_3O^- and 0.6 kcal/mol for $CD_3CD_2O^-$, compared to the unlabeled compounds, in excellent agreement with the value measured by Dang et al. [27].

DeFrees et al. [38] used the equilibrium method [41], to measure a normal secondary isotope effect for the methoxide system, an increase in the proton affinity of 0.5 ± 0.1 kcal/mol for CD_3O^- over CH_3O^-, in good agreement with the values measured by Haas and Harrison [26] and Grabowski et al. [37].

O'Hair et al. [28] used MIKES experiments to study the effect of isotopic substitution on the reactions of proton bound glycine dimers. They found an increase of 0.18 kcal/mol in the proton affinity for H_2NCD_2COOH compared to the unlabeled (k_H/k_D = 1.25), and an increase of 0.11 kcal/mol for $H_2{}^{15}NCH_2COOH$ (k_H/k_D = 1.14). Calculations of the zero-point vibrational energy at the HF/6-31G(d) level yielded a ΔPA value of 0.04 kcal/mol for H_2NCD_2COOH and 0.02 kcal/mol for $H_2{}^{15}NCH_2COOH$.

The present study deals with the effect of deuterium substitution on the properties of proton bound amine dimers, to examine the effect of the label position, size and structure of the proton bound dimer on the magnitude of the kinetic and thermodynamic secondary isotope effects and to investigate the effect of the deuterium substitution on the kinetic energy release (KER) for the dissociation of metastable proton bound amine dimers.

2. Experimental

The equilibrium and MIKES measurements were made with a high-pressure mass spectrometer constructed at the University of Waterloo configured around a VG 70-70 mass spectrometer whose configuration was changed from an E-B to a B-E instrument. The apparatus and its capabilities have been described in detail previously [42]. MIKES measurements were also performed with a JMS-HX110/HX110A mass spectrometer from JEOL, using low-pressure chemical ionization.

2.1. Equilibrium measurements

Gas mixtures were prepared (VG 70-70) in a temperature controlled 5-L stainless steel reservoir using methane as the high-pressure bath gas which served as the inert third body stabilization species to a pressure of 1200–1300 Torr, and which also served as the chemical ionization (CI) reagent gas. Other components of the mixture were present at pressures between 0.02 and 4.5 Torr. Trace amounts of carbon tetrachloride (electron scavenger) was added to the mixture. The gas mixture was bled into the ion source through a heated stainless steel inlet line to a pressure of 6.5–13 Torr. Ionization was accomplished by a 0.05–2-ms pulse of 2-keV electrons focused into the ion source through a 150-μm aperture. The ions

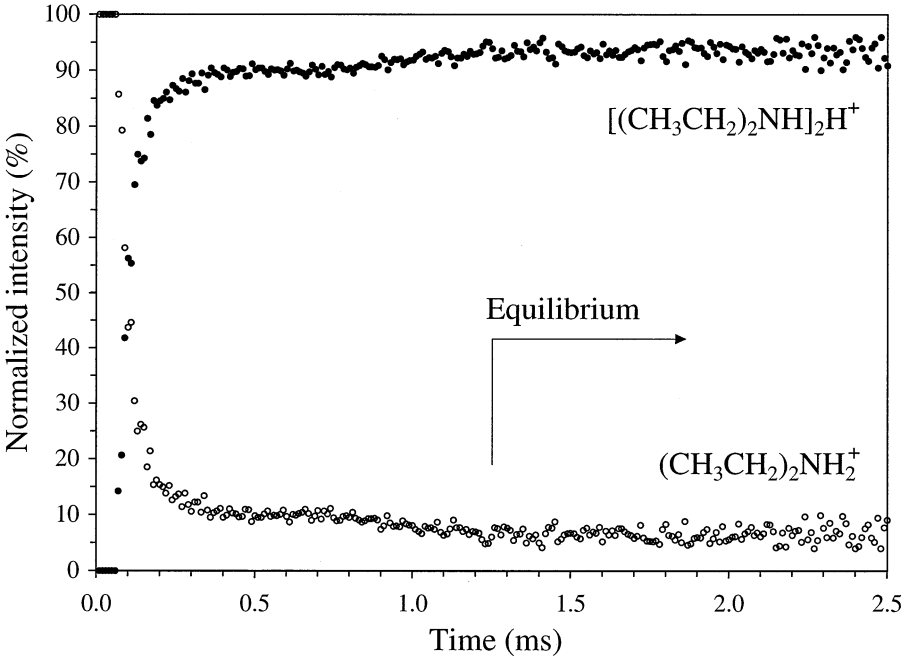

Fig. 1. Variation of normalized ionic abundance of $(CH_3CH_2)_2NH_2^+$ and its $(CH_3CH_2)_2NH$ adduct as a function of time after a 700-μs electron beam pulse. The result of 3000 electron gun pulses were accumulated at an ion source pressure of 6.5 Torr. Mixture composition: CH_4 (1239 Torr), $(CH_3CH_2)_2NH$ (800 mTorr) at 374 K (101 °C). Instrument: VG 70-70.

diffuse out of the ion source through a 150-μm aperture into the source chamber where the pressure is 50 μTorr. The ions are then accelerated towards the first cone through a 50–150-volt potential drop, where they enter the ion optics region and are accelerated up to 2.9 keV. The signal was monitored by a PC-based multichannel scaler signal acquisition system configured at 10–100-μs dwell time per channel. A total of 250 channels were acquired using a duty cycle of ~10 ms greater than the most persistent ion, which prevents pulse-to-pulse carry over in ion abundance. The results of 2000–20 000 electron gun pulses were accumulated, dependent on the signal intensity. Representative data are shown in Fig. 1 for the association reaction of $(CH_3CH_2)_2NH_2^+$ with $(CH_3CH_2)_2NH$.

2.2. MIKES measurements

The same gas mixtures were used for the MIKES measurements, and were bled into the ion source to a pressure of 15 Torr. Ionization was accomplished by a continuous beam of 2-keV electrons. Mass-selected ions were analyzed with a 70° (20 cm) electric sector allowing the parent ions to pass at 232 V. The signal was monitored by the same PC-based multichannel scaler signal acquisition system, but configured at a 9.8-ms dwell time per channel. A total of 1000 channels were acquired and 500 scans were accumulated. Representative data are shown in Fig. 2 for the spontaneous dissociation of the metastable proton bound dimer of CH_3CN and CD_3CN.

With the JMS-HX110/HX110A mass spectrometer ionization was accomplished by chemical ionization using methane as ionization gas at a ~0.5 Torr ion source pressure. The ions are then accelerated up to 10 keV, and reactions that take place in the third field free region of the mass spectrometer are studied. Between 2–1500 scans were accumulated, dependent on the signal intensity. Representative data are shown in Fig. 3 for the spontaneous dissociation of the metastable proton bound dimer of CH_3CN and CD_3CN. As is evident Fig. 2 and Fig. 3 give contra-

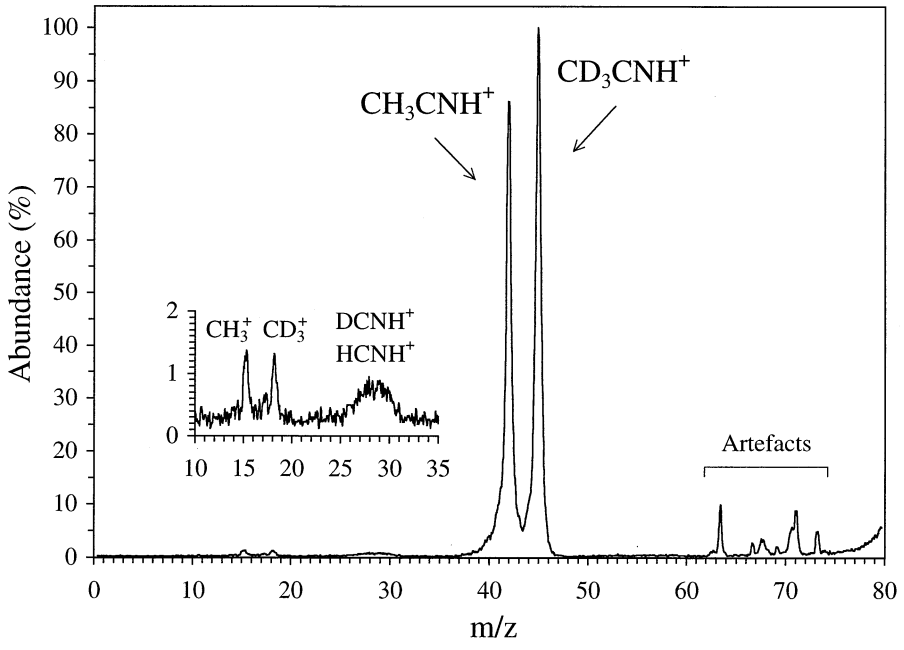

Fig. 2. MIKE spectrum of the proton bound dimer of CH_3CN and CD_3CN. The result of 500 electric sector scans were accumulated. Instrument: VG 70-70.

dictory data. This phenomenon is discussed later in the article.

2.3. Ab initio calculations

All electronic structure calculations were carried out using the GAUSSIAN94 series of programs [43]. The proton affinity differences between B and B-d_n compounds were derived from vibrational frequencies calculated at the MP2/6-31G(d,p) level. The scale factors suggested by Scott and Radom [44] were used.

2.4. Syntheses

All materials not commercially available were synthesized (Table 1). The purity and identity of the synthesized and commercial products were ascertained with ^{13}C-NMR and MS (EI and CI). Only negligible traces of impurities were found. All amines were prepared as the hydrochlorides and released with moist sodium hydroxide prior to the measurement.

3. Results and discussion

The dissociation reactions of proton bound amine dimers were investigated using pulsed ionization high-pressure mass spectrometry (PHPMS), Eqs. (5–7). The equilibrium constant was measured as a function of temperature and van't Hoff plots were constructed. Representative van't Hoff plots are shown in Fig. 4 for the $CD_3CH_2NH_2$ systems. Reaction enthalpies ($\Delta H°$) and reaction entropies ($\Delta S°$) were extracted from the van't Hoff plots and tabulated in Table 2.

$$(B)_2H^+ \rightleftarrows BH^+ + B \quad (5)$$

$$(B)(B\text{-}d_n)H^+ \rightleftarrows B + BH^+\text{-}d_n \quad (6)$$

$$(B\text{-}d_n)_2H^+ \rightleftarrows BH^+\text{-}d_n + B\text{-}d_n \quad (7)$$

As is evident from Table 2 the enthalpy of dissociation (the bonding energy) is observed to diminish as the size of the amines increases, as a result of weakened hydrogen bonding caused by the increased

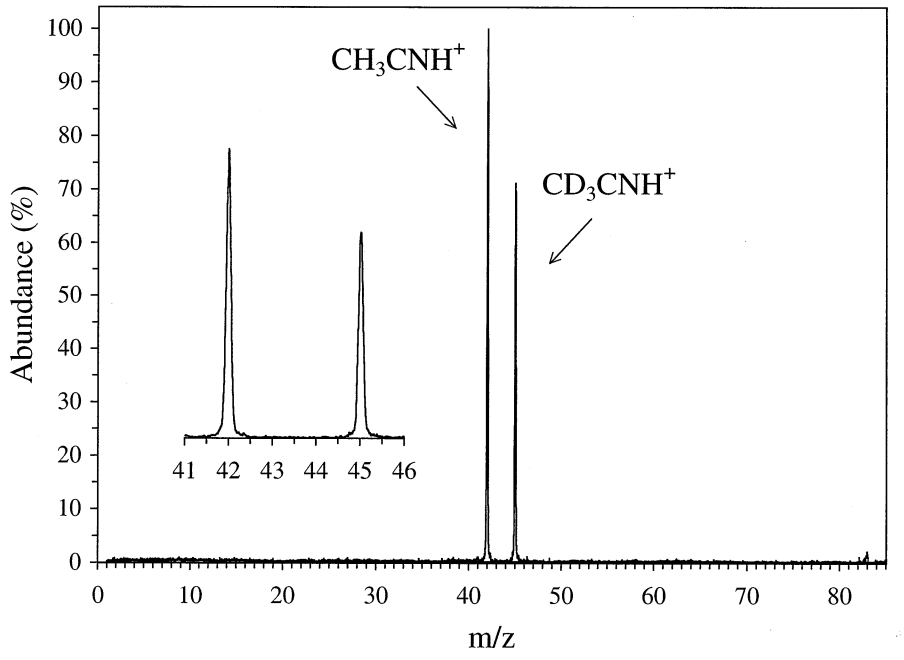

Fig. 3. MIKE spectrum of the proton bound dimer of CH_3CN and CD_3CN. The result of 17 electric sector scans were accumulated. Instrument: JMS-HX110/HX110A.

polarizability. A higher polarizability of the amine will, because of the inductive effect, result in a less positive partial charge on the bonding proton, which will weaken the ion-dipole interaction. No similar trend is observed for the entropy of dissociation, which is probably because of the considerable uncertainty associated with these values (± 3.0 cal/mol·K, because of the uncertainty of the partial pressures). A small isotope effect on the enthalpy of dissociation is observed (~0.1 kcal/mol) when Eqs. (5) and (6) and Eqs. (6) and (7) are compared, as well as a small isotope effect on the entropy of dissociation. When comparing Eqs. (5) and (7) an isotope effect of ~1 cal/mol·K is observed, which would lead one to predict an isotope effect of ~0.5 cal/mol·K when comparing Eqs. (5) and (6). Because of the difference in symmetry numbers between $(B)(B\text{-}d_n)H^+$ and $(B)_2H^+$ or $(B\text{-}d_n)_2H^+$, this value is counterbalanced by $R\cdot\ln 2$, which should give an observed $\Delta S°$ value for Eq. (6) which is ~1 cal/mol·K smaller than Eq. (5). This is consistent with our observations. There is no apparent (or detectable) effect of the label position, size or structure of the proton bound dimer on the isotope effect with respect to $\Delta H°$ or $\Delta S°$. These results suggest that the proton exchange between the labeled and unlabeled amines should show normal isotope effects with regard to the enthalpy of proton exchange, whereas no trend is expected to be detectable for the entropy of proton exchange because of the large uncertainty on $\Delta S°$.

The proton exchange reactions between labeled and unlabeled amines were investigated using PHPMS, Eq. (8); the equilibrium constant was measured as a function of temperature and van't Hoff plots constructed. A representative van't Hoff plot is shown in Fig. 5 for the $CH_3CD_2NHCH_3$ system. Reaction enthalpies and reaction entropies were extracted from the van't Hoff plots.

$$BH^+\text{-}d_n + B \rightleftarrows B\text{-}d_n + BH^+ \quad (8)$$

The reaction enthalpies cluster around 0.2 kcal/mol with a spread of ± 0.1 kcal/mol with no obvious pattern, which is to say that normal isotope effects are

Table 1
Synthesized compounds

Reactant	Reactant	Product	Ref.[a]
$C_2H_5OCONHCH_3$	$LiAlD_4$	CD_3NHCH_3	[45–47]
CD_3CN	$LiAlH_4$	$CD_3CH_2NH_2$	[48–50]
CH_3CN	$LiAlD_4$	$CH_3CD_2NH_2$	[48–51]
$CD_3CONHCH_3$	$LiAlH_4$	$CD_3CH_2NHCH_3$	[52]
$CH_3CONHCH_3$	$LiAlD_4$	$CH_3CD_2NHCH_3$	
$C_2H_5OCONHCH_2CH_3$	$LiAlD_4$	$CH_3CH_2NHCD_3$	[53]
$CD_3CONHCH_2CH_3$	$LiAlH_4$	$CD_3CH_2NHCH_2CH_3$	[48]
$CH_3CONHCH_2CH_3$	$LiAlD_4$	$CH_3CD_2NHCH_2CH_3$	[48,53]
$C_2H_5OCONHCH_2CH_2CH_3$	$LiAlD_4$	$CD_3NHCH_2CH_2CH_3$	[54,55]
$C_2H_5OCONHCH_2CH_2CH_2CH_3$	$LiAlD_4$	$CD_3NHCH_2CH_2CH_2CH_3$	
$C_2H_5OCON(CH_3)_2$	$LiAlD_4$	$CD_3N(CH_3)_2$	[56]
$(CD_3)_2NH$	$HCOOH/CH_2O/H_2O$	$(CD_3)_2NCH_3$	[56]
$(CD_3)_2NCDO$	$LiAlD_4$	$(CD_3)_3N$	[56–59]
$(CD_3O)_2Mg$	CD_3OH	CD_3OCH_3	[60][b]
CH_3OH	Mg	$(CH_3O)_2Mg$	
C_2H_5OCOCl	RNH_2[c]	$C_2H_5OCONHR$[c]	
CX_3COCl[d]	RNH_2[e]	CX_3CONHR[e]	
C_2H_5OCOCl	$HN(CH_3)_2$	$C_2H_5OCON(CH_3)_2$	

[a] Examples of alternative and identical synthetic procedures from the literature.
[b] Refers to the syntheses of the unlabeled compound.
[c] R = CH_3, C_2H_5, n-C_3H_7 or n-C_4H_9.
[d] X = H or D.
[e] R = CH_3 or C_2H_5.

observed (as expected) for the enthalpy of proton exchange. The observed entropy of proton exchange likewise appears random and unsystematic. There is no apparent (or detectable) effect of the label position, size or structure of the amine on the isotope effect with respect to ΔH° or ΔS°. These results suggest that the deuterium labeled amines have $\sim 0.2 \pm 0.1$ kcal/mol higher proton affinity than the nondeuterium labeled amines. It is often a good assumption to take ΔH° and ΔS° as independent of the temperature, however the ΔH° values for the proton exchange reactions studied here are so small that the temperature dependence could be significant. In that case the ΔH° values represent mean values with respect to the temperature interval studied. If there indeed is an effect of the size or structure of the amine on the ΔH°, this experiment is not sufficiently sensitive to detect it, but ab initio computed ΔH° values should be accurate enough to provide information about whether or not the size or structure is important.

The proton exchange reactions, Eq. (8), were studied using ab initio theory. The vibrational frequencies were computed and $\Delta H^\circ_{\text{theo}}$ (298 K) values calculated and tabulated in Table 3. If the isotopic substitution influences only the zero-point vibrational frequencies, the enthalpy of proton exchange (at 0 K) will reflect ΔZPE ($= \text{ZPE}_{2a} + \text{ZPE}_{2b} - \text{ZPE}_{2c} - \text{ZPE}_{2d}$, Fig. 6). The results in Table 3 predict that normal isotope effects should be observed for the enthalpy of proton exchange, consistent with the experimental results. The results clearly show an effect of the label position and the structure of the amine on the isotope effect with respect to ΔH°(ΔZPE). The magnitudes of the calculated ΔH° values are only a factor of ~ 2 smaller than the experimental ΔH° values, and the trends are qualitatively similar.

The effect of the ion source temperature on ΔH° and ΔS° has been computed. For the large amines ΔH° decreases $\sim 5\%$ from 300–700 K. The smaller

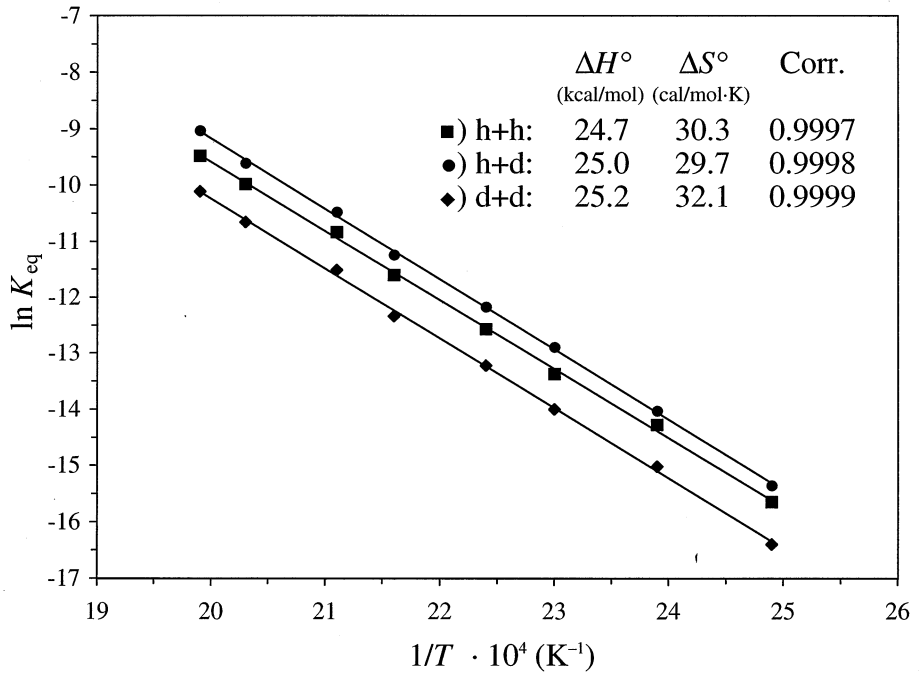

Fig. 4. van't Hoff plot for dissociation of the proton bound dimer of: $CH_3CN_2NH_2$ ($h + h$), $CH_3CH_2NH_2$ and $CD_3CH_2NH_2$ ($h + d$) and $CD_3CH_2NH_2$ ($d + d$). Instrument: VG 70-70.

Table 2
$\Delta H^{\circ a}$ and $\Delta S^{\circ a}$ for dissociation of proton bound amine dimers [Eqs. (5)–(7)]

	Eq. (5)		Eq. (6)		Eq. (7)	
B-d_n	$\Delta H^{\circ b}$ (kcal/mol)	$\Delta S^{\circ c}$ (cal/mol·K)	$\Delta H^{\circ b}$ (kcal/mol)	$\Delta S^{\circ c}$ (cal/mol·K)	$\Delta H^{\circ b}$ (kcal/mol)	$\Delta S^{\circ c}$ (cal/mol·K)
CD_3NH_2	26.8	34.9	26.9	33.9	27.0	36.0
CD_3NHCH_3	25.7	33.6	25.8	33.1	26.0	34.7
$CD_3CH_2NH_2$	24.7[d]	30.3[d]	25.0	29.7	25.2	32.1
$CH_3CD_2NH_2$	24.8[e]	29.9[e]	25.3	29.2	25.4	32.6
$CD_3CH_2NHCH_3$	24.0[f]	30.5[f]	24.1	29.6	24.2	31.4
$CH_3CD_2NHCH_3$	24.0[g]	30.4[g]	24.0	29.1	24.2	31.4
$CH_3CH_2NHCD_3$	23.9[h]	30.4[h]	24.0	29.4	24.2	31.6
$CD_3CH_2NHCH_2CH_3$	23.6[i]	33.7[i]	23.7	32.7	23.9	35.0
$CH_3CD_2NHCH_2CH_3$	23.7[j]	34.1[j]	23.8	33.1	24.0	35.0

[a] Measured on VG 70-70 (high-pressure ionization).

[b] The estimated relative uncertainty along a row is ± 0.05 kcal/mol, ± 0.1 kcal/mol down a column and the absolute uncertainty is estimated to 1.0 kcal/mol.

[c] The estimated relative uncertainty along a row is ± 0.5 cal/mol·K, ± 5.0 cal/mol·K down a column and the absolute uncertainty is estimated to ± 5.0 cal/mol·K.

[d–e] Replicated measurements.

[f–h] Replicated measurements.

[i–j] Replicated measurements.

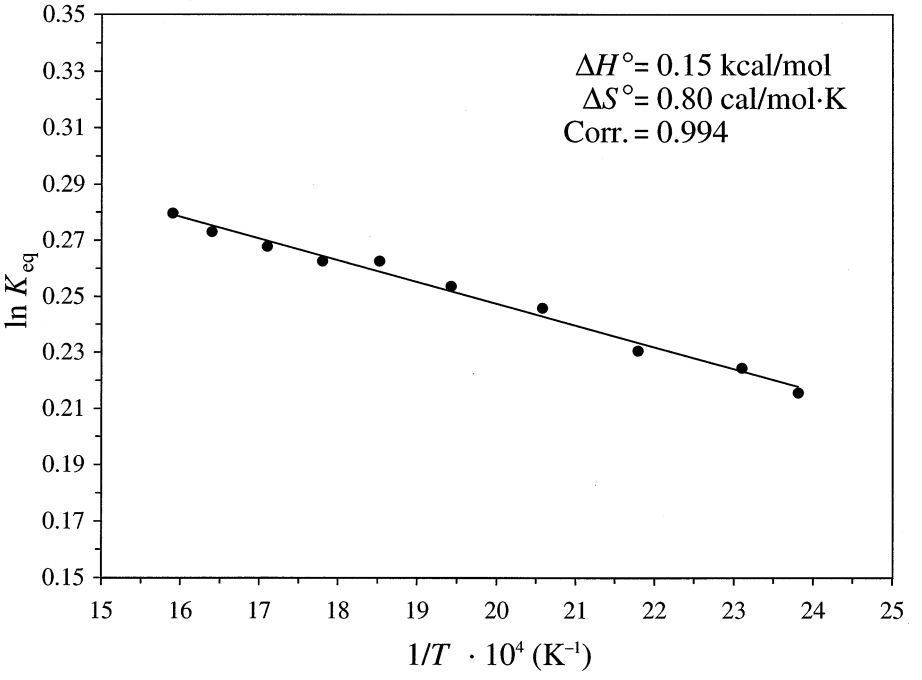

Fig. 5. van't Hoff plot for proton exchange between $CH_3CD_2NHCH_3$ and $CH_3CH_2NHCH_3$. Instrument: VG 70-70.

the size of the amine, the greater effect of the temperature on $\Delta H°$, so methylamine represents the system which is affected most. For methylamine $\Delta H°$ decreases 14% from 300–700 K. The same trend is observed for $\Delta S°$ (for all systems), but the change is insignificantly small. The computed $\Delta S°$ values for all temperatures are very close to 0 cal/mol·K (≥ -0.02 and ≤ 0.02 cal/mol·K). The effect of temperature on $\Delta H°$ and $\Delta S°$ for proton exchange is small, and for the experimentally determined $\Delta H°$ values the effect is insignificant when the accuracy of the experiment is considered.

The results in Table 3 show that the influence of deuterium labeling on the relative proton affinity is: α-$d_3 > \alpha$-$d_2 > \beta$-d_3, which is a rational result. The computational results for the proton exchange suggests that the label position in turn will influence the kinetic isotope effects for the dissociation reaction. The experimental and computational results suggest that normal kinetic isotope effects should be observed for the dissociation reaction, Eq. (9).

$$BH^+ + B\text{-}d_n \underset{m^*}{\overset{k_D}{\leftarrow}} (B)(B\text{-}d_n)H^+ \underset{m^*}{\overset{k_H}{\rightarrow}} B + BH^+\text{-}d_n \quad (9)$$

Dissociation reactions of proton bound amine dimers, Eq. (9), have been studied using MIKES. The

Table 3
$\Delta H°_{theo}$[a] (ΔPA_{theo})[a] (298 K) for proton exchange between deuterium labeled and unlabeled amines [Eq. (8)]

B-d_n	R = H	R = CH_3	R = C_2H_5	R = n-C_3H_7	R = n-C_4H_9
CD_3NH–R	0.12	0.12	0.12	0.12	0.12
CH_3CD_2NH–R	0.09	0.10	0.09	[b]	[b]
CD_3CH_2NH–R	0.03	0.03	0.03	[b]	[b]

[a] In kcal/mol. Calculated at the MP2/6-31G(d,p) level. Frequencies are scaled [44].
[b] Not computed.

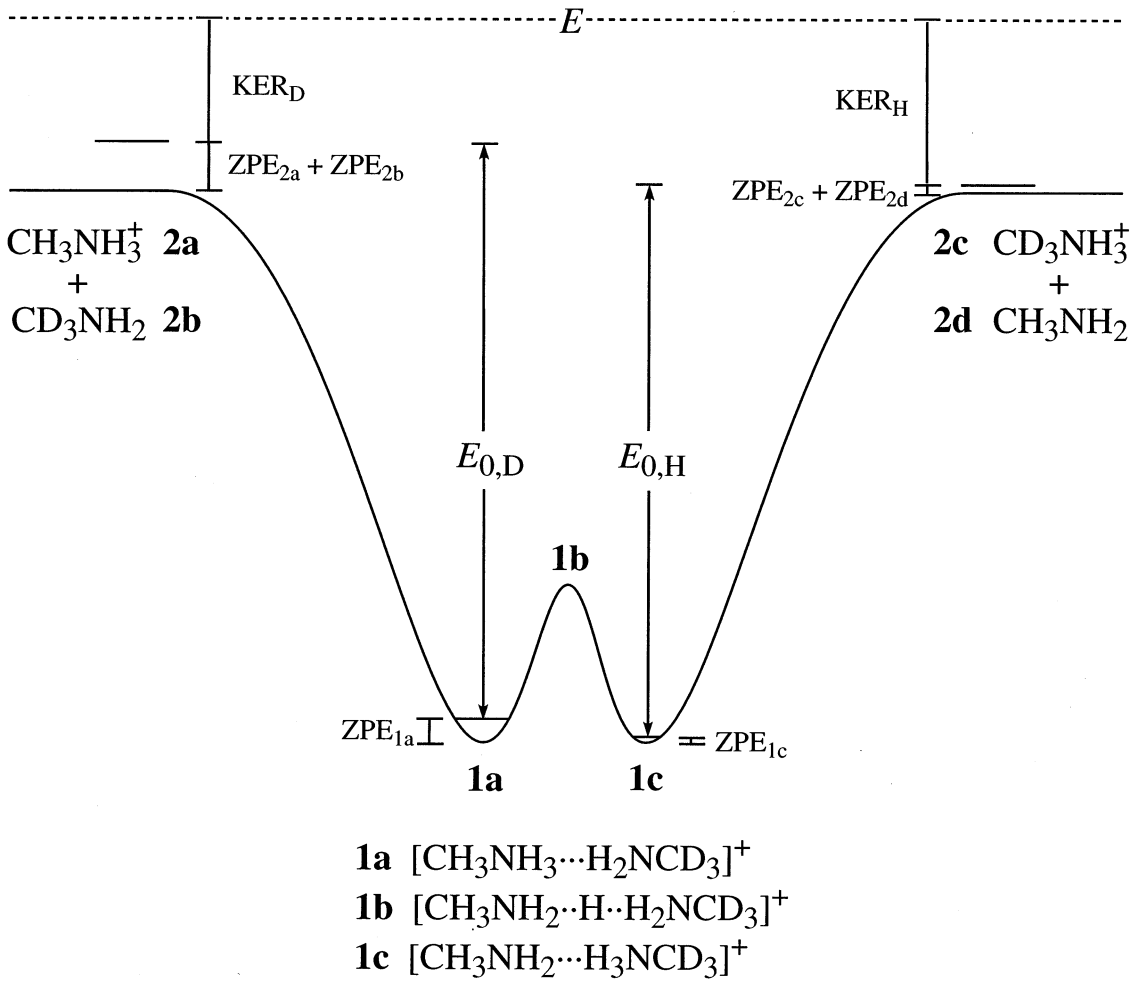

Fig. 6. Schematic energy profile (not drawn to scale) for association, intramolecular proton transfer and dissociation. ΔZPE (proton exchange between **2b** and **2d**) = $ZPE_{2c} + ZPE_{2d} - ZPE_{2a} - ZPE_{2b}$. $E_{0,D}$ and $E_{0,H}$ are the activation energies for dissociation of the proton bound dimer, **1a–c**. **1b** is the transition state for intramolecular proton transfer.

Table 4
k_H/k_D[a] for dissociation of deuterium labeled metastable proton bound amine dimers [Eq. (9)]

B-d_n	R = H	R = CH_3	R = C_2H_5	R = n-C_3H_7	R = n-C_4H_9
CD_3NH–R	4.1 ± 0.1	1.63 ± 0.05	1.36 ± 0.01	1.30 ± 0.01	1.26 ± 0.02
CH_3CD_2NH–R	1.30 ± 0.01	1.24 ± 0.01	1.25 ± 0.01	[b]	[b]
CD_3CH_2NH–R	1.18 ± 0.01	1.13 ± 0.01	1.13 ± 0.01	[b]	[b]

[a] Measured on JMS-HX110/HX110A (low-pressure ionization).
[b] Not measured.

Table 5
k_H/k_D[a] for dissociation of deuterium labeled metastable proton bound amine dimers [Eq. (9)]

B-d_n	R = H	R = CH_3	R = C_2H_5	R = n-C_3H_7	R = n-C_4H_9
CD_3NH–R	1.39 ± 0.01	1.28 ± 0.01	1.22 ± 0.01	1.19 ± 0.01	1.16 ± 0.01
CH_3CD_2NH–R	1.16 ± 0.01	1.14 ± 0.01	1.12 ± 0.01	[b]	[b]
CD_3CH_2NH–R	1.17 ± 0.01	1.15 ± 0.01	1.13 ± 0.01	[b]	[b]

[a] Measured on VG 70-70 (high-pressure ionization).
[b] Not measured.

kinetic isotope effects were measured on two different mass spectrometers and tabulated in Table 4 (JMS-HX110/HX110A, low-pressure ionization) and Table 5 (VG 70-70, high-pressure ionization). Normal isotope effects are observed for reactions occurring after both low and high-pressure ionization. This is consistent with the results from the equilibrium measurements and the ab initio calculations. The magnitude of the isotope effect for the dissociation reactions clearly depend on the label position, size and structure of the proton bound dimer. The differences between the kinetic isotope effects measured on the two instruments (Tables 4 and 5) illustrate the difference in internal energies of the reacting ions in the two instruments used. The difference between the critical energies of the two dissociation reactions (Fig. 6) will be less important for ions of higher internal energy, and will result in smaller kinetic isotope effects. The difference in internal energies is caused by the different ionization conditions and different ion lifetimes. Ions with a lifetime of 18–29 μs (for *m/z* 100) have been studied when using the JMS-HX110/HX110A mass spectrometer (Table 4), and ions with a lifetime of 15–19 μs (for *m/z* 100) have been studied when using the VG 70-70 mass spectrometer (Table 5). If the ionization conditions are assumed to be the same for the two instruments, the older ions (Table 4) should have lower internal energy, and should in turn result in higher kinetic isotope effects, which is consistent with Tables 4 and 5.

The kinetic isotope effects diminish with increasing number of degrees of freedom in the proton bound dimers. Reactions that take place in the field free regions in the mass spectrometer represents a very narrow ion lifetime window, that is, the observed reactions take place with the same rate. For a homologous series of parent ions undergoing the same type of reaction in a given field free region, the internal energy should increase with the number of degrees of freedom in order that the dissociation rate remain constant. This higher internal energy will result in a lower isotope effect. However larger proton bound dimers are also heavier, and heavier ions take longer to reach the field free region in the mass spectrometer. Furthermore, larger proton bound amine dimers are bound less strongly (Table 2). The degrees of freedom effect, the ion lifetime effect and the well depth effect will all influence the internal energy of the proton bound dimer. The overall variation for the proton bound dimers of CH_3NH–R and CD_3NH–R (R = H, CH_3, C_2H_5, n-C_3H_7 or n-C_4H_9) is illustrated in Fig. 7. The kinetic isotope effect (1.145 ± 0.010) for R = C_5H_{11} is empirically determined from the other points.

The kinetic isotope effect for $(CD_3NH_2)(CH_3NH_2)H^+$ measured under low-pressure ionization conditions (k_H/k_D = 4.1 ± 0.1, Table 4), is extraordinarily large relative to the other systems. Because this may reflect mass discrimination in the mass spectrometer, possibly related to the off-axis detector employed, the mass spectrometer was ascertained for mass discrimination. This yielded no observations that can explain the extraordinarily large kinetic isotope effect for the proton bound dimer of methylamine.

The results in Table 4 show that the influence of deuterium labeling on the relative proton affinity is: α-d_3 > α-d_2 > β-d_3, consistent with the results from the ab initio calculations. However the results for dissociation of ions formed by high-pressure

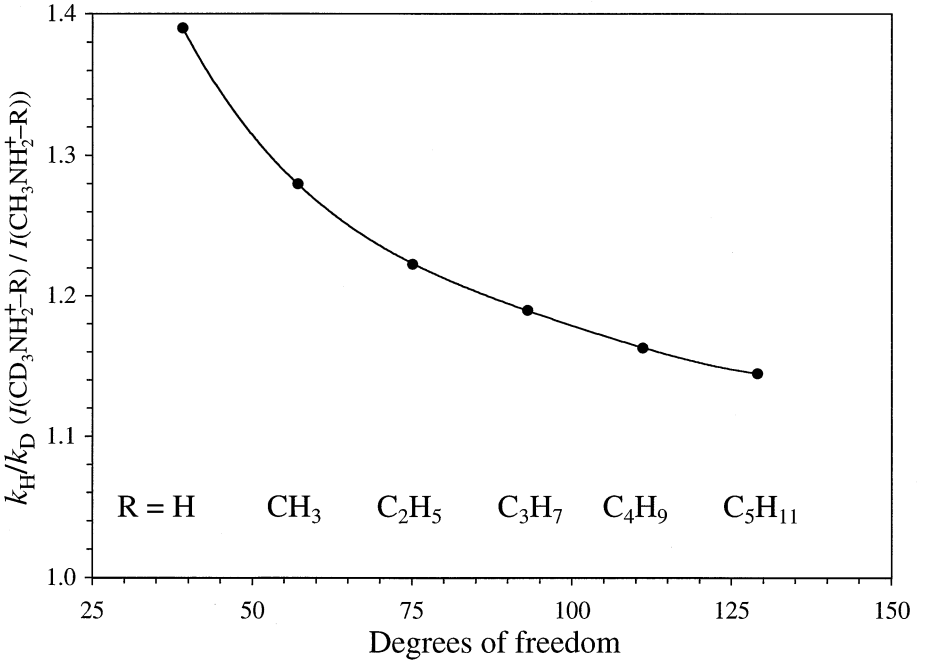

Fig. 7. The kinetic isotope effect for the dissociation of the metastable proton bound dimer of $CD_3NH–R$ and $CH_3NH–R$ as a function of the degrees of freedom of the proton bound dimer. Instrument: VG 70-70.

ionization (Table 5) indicate that the order is: α-d_3 > β-d_3 > α-d_2. The differences in the kinetic isotope effects (Table 5) for the $CH_3CD_2NH–R$ systems and the $CD_3CH_2NH–R$ systems correspond to the estimated uncertainty (± 0.01) of the measurement. It could therefore be argued that the observed relative proton affinity order (based on k_H/k_D) between the α-d_2 labeled and the β-d_3 labeled amines, is a coincidence. The estimate of the uncertainty is based on the results of repeated measurements, Table 6, at different ion source temperatures (to detect possible temperature dependence) and with two mixture compositions (to detect the presence of possible isobaric ions). All the systems have been tested like this, and no dependence of the ion source temperature or the mixture composition on the kinetic isotope effect, was observed. In order to further elucidate these influences on the relative proton affinity order for the α-d_2 and β-d_3 labeled amines (when measured on the VG 70-70 mass spectrometer), reactions corresponding to Eq. (10) have been studied on the VG 70-70 mass spectrometer for diethylamine.

$$BH^+\text{-}d_2 + \text{B-}d_3 \overset{m^*}{\leftarrow} (\text{B-}d_2)(\text{B-}d_3)H^+ \overset{m^*}{\rightarrow} (\text{B-}d_2) + BH^+\text{-}d_3 \quad (10)$$

From the MIKES spectrum, Fig. 8, it is clear (in spite of the poor resolution) that loss of the α-d_2 labeled

Table 6
k_H/k_D for dissociation of the metastable proton bound deuterium labeled methylamine dimer at various ion source temperatures and mixture compositions [Eq. (9), B = CH_3NH_2]

T^a (°C)	$I(CD_3NH_3^+)^b$ / $I(CH_3NH_3^+)$	$P(CD_3NH_2)^c$ / $P(CH_3NH_2)$
48	1.38	0.67
136	1.39	0.67
173	1.40	1.50
202	1.39	1.50
216	1.39	0.67
234	1.38	1.50

[a] Ion source temperature.
[b] Kinetic isotope effect (k_H/k_D) measured on VG 70-70 (high-pressure ionization).
[c] Partial pressure ratio.

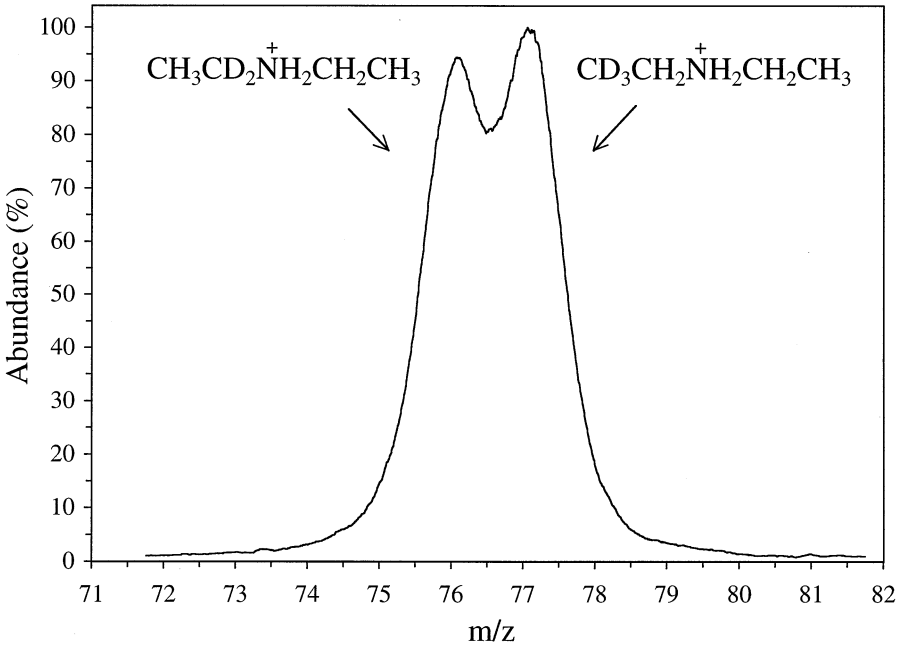

Fig. 8. MIKE spectrum of the proton bound dimer of $CH_3CD_2NHCH_2CH_3$ and $CD_3CH_2NHCH_2CH_3$. CI (CH_4) ionization. The result of 500 electric sector scans were accumulated. Instrument: VG 70-70.

amine from the proton bound dimer is favored (i.e. the α-d_3 labeled amine have the higher proton affinity), which is consistent with the observed trend in Table 5, but inconsistent with the observed trend in Table 3, where the α-d_3 labeled amines are calculated to have lower proton affinities. The same measurement has been done for all the α-d_2/β-d_3 systems on the JMS-HX110/HX110A mass spectrometer using low-pressure ionization, Table 7. The MIKES spectrum of the diethylamine system using low-pressure ionization is shown in Fig. 9. Here the loss of the α-d_3 labeled amine from the proton bound dimer is favored (i.e. the α-d_2 labeled amine have the higher proton affinity), which is consistent with the observed trend in Table 4, and furthermore consistent with the observed trend in Table 3, where the α-d_2 labeled amines are calculated to have higher proton affinities. There is clearly a discrepancy (compare Figs. 8 and 9) between the results obtained using low- or high-pressure ionization, with respect to the proton affinity order of the α-d_2 and β-d_3 labeled amines. Because the results obtained using low-pressure ionization are

Table 7
Relative product ion intensities for dissociation of metastable proton bound dimers of trideuterium labeled and dideuterium labeled amines [Eq. (10)]

B-d_3	B-d_2	$\frac{I(BH^+\text{-}d_2)^a}{I(BH^+\text{-}d_3)}$	$\frac{I(BH^+\text{-}d_2)^b}{I(BH^+\text{-}d_3)}$
$CD_3CH_2NH_2$	$CH_3CD_2NH_2$	1.04	1.10
$CD_3CH_2NHCH_3$	$CH_3CD_2NHCH_3$	1.10	1.10
$CH_3CH_2NHCD_3$	$CH_3CD_2NHCH_3$	0.92	0.91
$CD_3CH_2NHCH_2CH_3$	$CH_3CD_2NHCH_2CH_3$	1.09	1.11

[a] Measured on JMS-HX110/HX110A (low-pressure ionization). The uncertainty is ± 0.01.
[b] Indirect measurement [calculated from the B/B-d_n results, Eq. (9)].

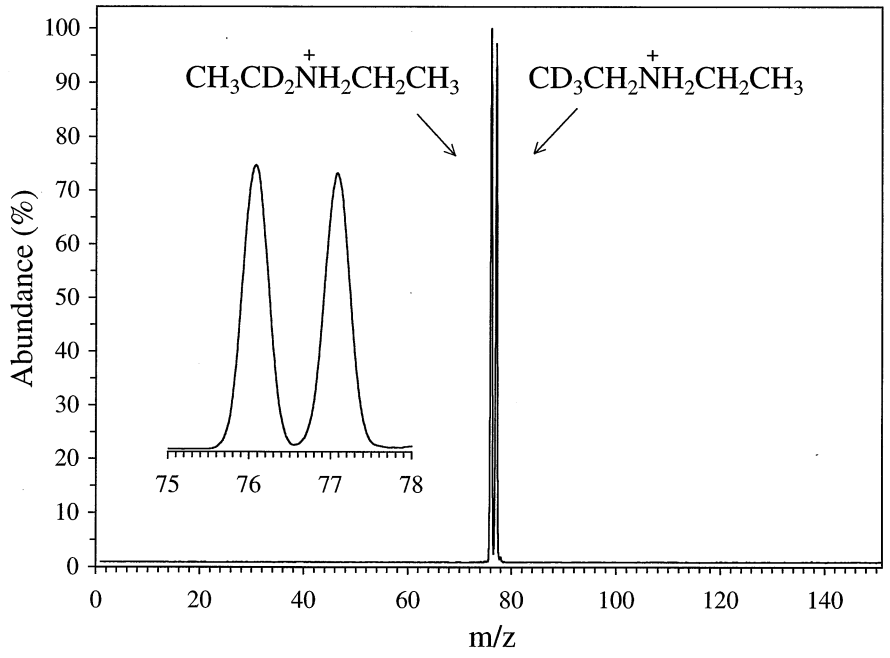

Fig. 9. MIKE spectrum of the proton bound dimer of $CH_3CD_2NHCH_2CH_3$ and $CD_3CH_2NHCH_2CH_3$. CI (CH_4) ionization. The result of two electric sector scans were accumulated. Instrument: JMS-HX110/HX110A.

qualitatively consistent with the results from the ab initio calculations, there may be special circumstances associated with performing the measurement using high-pressure ionization. An explanation for this phenomenon has not yet been found.

$CH_3CH_2NHCH_3$ represents a special system because it is the only amine (of the amines studied) which is labeled in three different positions ($CH_3CH_2NHCD_3$, $CH_3CD_2NHCH_3$ and $CD_3CH_2NHCH_3$). The proton bound dimers of the unlabeled amine and each of the labeled amines, have the same size (i.e. same number of degrees of freedom), the same structure, essentially the same binding energy (Table 2) and should therefore be expected to have the same effective temperature if Eq. (4) is considered to be valid. This should be the case when comparing any CD_3CH_2NH–R system with the corresponding CH_3CD_2NH–R system. From the measured k_H/k_D values (Tables 4 and 5) and the calculated ΔPA ($\Delta H^\circ_{theo.}$) values (Table 3), effective temperatures for (B)(B-d_n)H^+ can be calculated from Eq. (4). Doing so, it is found that the $CH_3CH_2NHCD_3$ system and the $CH_3CD_2NHCH_3$ system have similar effective temperatures, and that the $CD_3CH_2NHCH_3$ system seems to have a significantly lower effective temperature compared to the other two systems. All of the CD_3CH_2NH–R systems have effective temperatures that are significantly lower than the CH_3CD_2NH–R systems. The accuracy of the effective temperatures is determined by the validity of Eq. (4), the accuracy of the measured k_H/k_D values and the accuracy of the calculated ΔPA values. The k_H/k_D values (Tables 4 and 5) are very well determined (± 0.01 in most cases), so it is unlikely that this is the cause of the discrepancy. The accuracy of the calculated ΔPA values (Table 3) is not known. While small changes in the k_H/k_D values have an insignificant effect on the effective temperature, small changes in the ΔPA values have a large effect on the calculated effective temperature. This suggests that the ΔPA value could be poorly determined for the CD_3CH_2NH–R systems. The problem with this argument is that the calculated ΔPA values for these systems are all based on the same optimized structures

Table 8
T_{eff}[a] (K) for deuterium labeled metastable proton bound amine dimers [Eq. (9)]

B-d_n	R = H	R = CH_3	R = C_2H_5	R = n-C_3H_7	R = n-C_4H_9
CD_3NH–R	44 ± 1	128 ± 8	203 ± 5	238 ± 7	270 ± 17
CD_3CD_2NH–R	167 ± 5	204 ± 8	196 ± 7	[b]	[b]
CD_3CH_2NH–R	149 ± 7	202 ± 14	202 ± 14	[b]	[b]

[a]Measured on JMS-HX110/HX110A (low-pressure ionization). The uncertainty is based only on the uncertainty on k_H/k_D.
[b]Not measured.

of the neutral and the protonated amine, only the frequencies are different (i.e. the ZPEs). This means that the error because of the inadequacy of the level of theory can be expected to be the same for all of the systems. However assuming that the ΔPA value (0.03 kcal/mol) for some reason is poorly determined, the ΔPA value may be adjusted so that all of the CD_3CH_2NH–R and CH_3CD_2NH–R systems have approximately the same effective temperatures. An average effective temperature for the three $CH_3CH_2NHCH_3$ systems can be determined from a plot of ln k_H/k_D versus ΔPA (Eq. (4)). Using the corrected ΔPA value for the CD_3CH_2NH–R systems results in a straight line with a correlation coefficient of 0.992 and a effective temperature of 203 K if based on the values in Table 4, and a correlation coefficient of 0.988 and a effective temperature of 321 K if based on the values in Table 5. These average effective temperatures can be used to correct all of the calculated ΔPA values from Table 3 (because the ΔPA values are constant along a row). Based on the values in Table 4 and an average effective temperature of 203 K, the following results are obtained: $CH_3CH_2NHCD_3$ (0.124 kcal/mol), $CH_3CD_2NHCH_3$ (0.087 kcal/mol) and $CD_3CH_2NHCH_3$ (0.049 kcal/mol). Based on the values in Table 5 and an average effective temperature of 321 K, the following results are obtained: $CH_3CH_2NHCD_3$ (0.127 kcal/mol), $CH_3CD_2NHCH_3$ (0.084 kcal/mol) and $CD_3CH_2NHCH_3$ (0.089 kcal/mol).

From the measured k_H/k_D values (Tables 4 and 5) and the corrected ΔPA values, effective temperatures of (B)(B-d_n)H^+ have been calculated from Eq. (4), and tabulated in Table 8 (JMS-HX110/HX110A, low-pressure ionization) and in Table 9 (VG 70-70, high-pressure ionization). The so-called effective temperature (which is not an actual temperature) can be regarded as a measure of the internal energy [35]. If this is the case we should expect to see an increase in the effective temperature with increasing size of the reacting ion, i.e. an increase in the values along a row in Tables 8 and 9. This is indeed observed, such that the trend is qualitatively consistent with the argument in this sense. The CD_3NH–R systems (first row) have, as expected, lower effective temperatures compared to the CH_3CD_2NH–R systems (second row) because of the size difference. Because the accuracy of the calculated ΔPA values is not known, the reported uncertainties in Tables 8 and 9, are therefore based only on the accuracy of the measured k_H/k_D values.

Craig et al. [61] have described the effective temperature as the excess energy per mode of the proton bound dimer, Eq. (11), where s is the number of oscillators in the proton bound dimer.

Table 9
T_{eff}[a] (K) for deuterium labeled metastable proton bound amine dimers [Eq. (9)]

B-d_n	R = H	R = CH_3	R = C_2H_5	R = n-C_3H_7	R = n-C_4H_9
CD_3NH–R	194 ± 4	259 ± 8	321 ± 12	367 ± 16	431 ± 24
CH_3CD_2NH–R	285 ± 16	323 ± 21	373 ± 27	[b]	[b]
CD_3CH_2NH–R	285 ± 29	320 ± 18	366 ± 24	[b]	[b]

[a] Measured on VG 70-70 (high-pressure ionization). The uncertainty is based only on the uncertainty on k_H/k_D.
[b] Not measured.

Table 10
$E - E_0$[a] [kcal/mol, from Eq. (11)] for deuterium labeled metastable proton bound amine dimers [Eq. (9)]

B-d_n	R = H	R = CH_3	R = C_2H_5	R = n-C_3H_7	R = n-C_4H_9
CD_3NH–R	3.3 ± 0.1	14.2 ± 0.9	29.8 ± 0.8	43.5 ± 1.3	59.0 ± 3.7
CH_3CD_2NH–R	18.6 ± 0.5	30.0 ± 1.2	35.8 ± 1.3	[b]	[b]
CD_3CH_2NH–R	16.6 ± 0.8	29.7 ± 2.1	36.9 ± 2.6	[b]	[b]

[a] Measured on JMS-HX110/HX110A (low-pressure ionization). The uncertainty is based only on the uncertainty on T_{eff}.
[b] Not measured.

$$T_{eff} = \frac{E - E_0}{R(s-1)} \quad (11)$$

Assuming this expression is valid, it is now possible to convert the measured effective temperatures to excess energies, $E - E_0$, of the metastable proton bound dimers. This has been done for the effective temperatures measured using low-pressure ionization, Table 10. The excess energy can also be obtained from the measured KER associated with the reaction corresponding to Eq. (9). $T_{0.5}$ (half height peak width) were used as a measure of KER. The average values of KER_H and KER_D, measured using low-pressure ionization, has been multiplied by the number of modes in the proton bound dimer to give the excess energy, $E - E_0$, and tabulated in Table 11. When comparing the excess energies obtained from the relative peak heights (k_H/k_D, Eq. (9)), Table 10, with the excess energies obtained from the half height peak widths (KER_H and KER_D, Eq. (9)), Table 11, the former have values which are ~50% greater than the latter. The trend is clearly the same for the two sets of values. Considering the extent of data manipulation required to obtain the values in Table 10, the agreement is remarkably good. Furthermore, Eq. (11) is a limiting equation which applies best at high internal energies, which is not the situation for metastable ions.

The extent of deuterium substitution will affect the observed isotope effect (the isotope effects reported so far in this paper are simply the observed ion abundance ratios). This phenomenon has been studied for metastable proton bound dimers of $(CH_3)_3N$ and deuterium labeled trimethylamines, Eq. (9). The kinetic isotope effects of the reactions of the proton bound dimers of $(CH_3)_3N$ and $CD_3N(CH_3)_2$, $(CD_3)_2NCH_3$, or $(CD_3)_3N$ have been measured; the dimer ions were formed by high-pressure ionization. It was not possible to form the proton bound dimers using low-pressure ionization. The $CD_3N(CH_3)_2$ system showed a temperature and mixture composition dependence on the kinetic isotope effect, which suggests the presence of isobaric ions. Loss of HD from $CD_3NH(CH_3)_2^+$ (in the ion source) generates $CD_2 = N(CH_3)_2^+$, which is isobaric with $NH(CH_3)_3^+$. As an alternative to this system we can consider the $CD_3NHCH_2CH_3$ system, for which HD loss is negligible. The preferred way to convert the observed isotope effect to isotope effect per deuterium is to take the n^{th} root of the isotope effect, were n is the number of deuteriums. The validity of this procedure has been

Table 11
$E - E_0$[a] (kcal/mol, from KER) for deuterium labeled metastable proton bound amine dimers [Eq. (9)]

B-d_n	R = H	R = CH_3	R = C_2H_5	R = n-C_3H_7	R = n-C_4H_9
CD_3NH–R	2.2 ± 0.5	9.9 ± 0.6	19.6 ± 0.9	28.2 ± 1.1	39.3 ± 1.3
CH_3CD_2NH–R	11.8 ± 0.7	19.6 ± 0.9	28.4 ± 1.1	[b]	[b]
CD_3CH_2NH–R	12.3 ± 0.7	19.7 ± 0.9	29.6 ± 1.1	[b]	[b]

[a] Measured on JMS-HX110/HX110A (low-pressure ionization). KER = $(KER_H + KER_D)/2$. The uncertainty is based on an estimated uncertainty on $T_{0.5}$ of ± 0.5 meV.
[b] Not measured.

tested. The kinetic isotope effect measured for the $CD_3NHCH_2CH_3$ system is 1.22 ± 0.01 (Table 5), which gives a value of 1.069 ± 0.003 per deuterium. The $(CD_3)_2NCH_3$ system gives an observed kinetic isotope effect of 1.52 ± 0.01, which results in a value of 1.072 ± 0.001 per deuterium. Finally the $(CD_3)_3N$ system gives an observed kinetic isotope effect of 2.03 ± 0.01, which corresponds to a value of 1.082 ± 0.001 per deuterium. The three values are within acceptable range of each other, which thus supports the use of the procedure.

The dissociation of proton bound amine dimers was also investigated to study the effect of deuterium labeling on the KER. Reactions corresponding to Eq. (9) and Eqs. 12 and 13 were studied on the JMS-HX110/HX110A mass spectrometer (low-pressure ionization).

$$(B)_2H^+ \overset{m^*}{\rightarrow} BH^+ + B \quad (12)$$

$$(B\text{-}d_n)_2H^+ \overset{m^*}{\rightarrow} BH^+\text{-}d_n + B\text{-}d_n \quad (13)$$

The KERs are small (2–16 meV) and increase with the size of the proton bound amine dimer. Small KERs are often an indication of a simple cleavage of the hydrogen bond, as opposed to large KERs, which suggest that rearrangement be involved in the reaction. Metastable proton bound amine dimers have simple cleavage as the only reaction pathway.

Lund and Bojesen [62] studied the degrees of freedom effect on the dissociation of proton bound dimer systems, and observed that larger dimers yield larger KERs. They also studied a group of isobaric amines, and found that the enthalpy of dissociation decreases with increasing proton affinity within the group (this is not consistent with the result from our measurements for ethylamine and dimethylamine, Table 2). Because the critical energies for the association reaction are negligible, the critical energies for the dissociation reaction are equal to the enthalpy of dissociation. The excess energy must then decrease to the same extent that the critical energy decreases, in order for the reaction rate to remain constant. Because the excess energy and the critical energy decrease by the same fraction, the difference must then also decrease, and thus, decrease the KER, in agreement with their observations. They furthermore found that for a group of isobaric amines the KER constitutes the same fraction (~10%) of the enthalpy of dissociation.

Two procedures were used to study the effect of deuterium labeling on the KER for dissociation of metastable proton bound amine dimers. The KER for reactions given by Eq. (12) has been compared with the KER for reactions given by Eq. (13). Doing this the KER_H/KER_D ratios are observed to cluster around 1.00. The experiments are obviously not sensitive enough for two independent measurements to be compared. To detect the presumably small effect of the deuterium substitution on KER, a single experiment is needed like the reaction corresponding to Eq. (9). Doing so all the KER_H/KER_D ratios are observed to be slightly greater than 1 (the average KER_H/KER_D ratio is 1.02), which suggests that a subtle effect of the deuterium substitution on the KER might exist. Thus, with loss of the unlabeled amine from the proton bound dimer, $(B)(B\text{-}d_n)H^+$, one expects higher KERs because $KER_H/KER_D > 1$. The experiment is clearly not sensitive enough for any possible trends to be observed, so it is not possible to determine if the label position, size or structure of the proton bound dimer is important. Once again the methylamine system shows an abnormal behavior, with an unusually large KER_H/KER_D value of 1.31 (Eq. (9)). This is probably linked to the unusually large kinetic isotope effect for this system under the conditions in question.

The smallest systems from other compound classes have been studied in the same way, though not systematically. The results are presented in Table 12. When produced from high-pressure ionization, the proton bound dimer of $(CH_3)_2CO$ and $(CD_3)_2CO$ were seen to dissociate such that the relative ratios of the product ions was dependent on the ion source temperature. This suggests special circumstances. The proton bound dimer of acetone is subject of an ongoing study, which will be reported at a later date.

The acetonitrile system also shows an abnormal behavior. ΔPA_{exp} (−0.4 kcal/mol), ΔPA_{theo} (−0.07 kcal/mol), k_H/k_D (0.65, low-pressure ionization, Fig. 3) and KER_H/KER_D (0.88) show an inverse isotope effect, but k_H/k_D using high-pressure ionization show

Table 12
Results from analogue studies of deuterium labeled proton bound dimers of other compound classes

B-d_n	ΔPA_{exp}[a] (kcal/mol)	ΔPA_{theo}[b] (kcal/mol)	k_H/k_D[c]	k_H/k_D[d]	$\frac{KER_H}{KER_D}$[c]	T_{eff}[c,e] (K)	T_{eff}[d,e] (K)
CD_3NH_2	0.3 ± 0.1	0.12	4.1 ± 0.1	1.39 ± 0.01	1.31	44 ± 1	194 ± 4
CD_3OH	0.3 ± 0.1	0.12	2.02 ± 0.02	1.19 ± 0.01	1.08	86 ± 1	347 ± 16
CD_3OCH_3	0.3 ± 0.1	0.12	1.33 ± 0.02	1.18 ± 0.01	1.02	212 ± 11	365 ± 18
CD_3CN	−0.4 ± 0.1	−0.07	0.65 ± 0.04	1.10 ± 0.02	0.88	82 ± 13	370 ± 59
$(CD_3)_2CO$	0.0[f] ± 0.1	−0.03	0.99 ± 0.01	[g]	0.99	1502 ± 755	[g]

[a] (8). Measured on VG 70-70 (high-pressure ionization).
[b] (8). Calculated at the MP2/6-31G(d,p) level. Frequencies are scaled [44].
[c] (9). Measured on JMS-HX110/HX110A (low-pressure ionization).
[d] (9). Measured on VG 70-70 (high-pressure ionization).
[e] Based on ΔPA_{theo}. The uncertainty is based only on the uncertainty on k_H/k_D.
[f] Measured by Dr. J.E. Szulejko, University of Waterloo.
[g] The relative signal intensity is dependent on the ion source temperature.

a normal kinetic isotope effect (1.10, Fig. 2). There may be special circumstances associated with the measurement of k_H/k_D using high-pressure ionization, because this observation is clearly inconsistent with the other observations for this system. Mass discrimination has, as discussed earlier, been excluded as a possible source of error. To ensure that these observations were not caused by an interfering memory effect in the reservoir, the measurement was reproduced 15 months later on the same instrument with new acetonitrile and acetonitrile-d_3. The same result was obtained. The CI mass spectrum obtained on the JMS-HX110/HX110A instrument (low-pressure ionization) shows peaks only from the protonated monomers, dimers and trimers. The CI mass spectrum obtained on the VG 70-70 instrument using high-pressure ionization at an ion source temperature of 24 °C, shows peaks from the proton bound monomers, dimers and trimers, clusters between three acetonitrile molecules and protonated water, methylated clusters of two acetonitrile molecules and one water molecule, and ethylated dimers and trimers. The MIKES spectra from both instruments show a negligible amount of deuterium exchange (m/z 41, 43 and 44) in the proton bound dimer, and minor peaks (< 1%) from CH_3^+, CD_3^+, $HCNH^+$ and $DCNH^+$. Deuterium exchange will result in the opposite effect, i.e. decrease the CD_3CNH^+ signal and to a lesser extent increase the CH_3CNH^+ signal. The main difference between the MIKES experiments performed on the two instruments is the amount of internal energy in the metastable proton bound dimer. The discrepancy is seen for the experiment where the metastable proton bound dimers have a relative large amount of internal energy. If an entropy effect is dominant at high internal energies, this phenomenon should be revealed from ab initio calculations. According to the ab initio calculations, the protonation of CH_3CN, compared to CD_3CN, is entropically more favored at low internal energies, consistent with the observation of an inverse kinetic isotope effect. The computed $\Delta S°$ values in the ion source temperature range between 300–700 K are all negative, which means that the protonation of CD_3CN will not be entropically favored at any temperature. In order to find out whether changing the internal energy in the two MIKES experiments results in the same qualitatively behavior, the two experiments have been performed using different acceleration voltages. The kinetic isotope effect decreases when the acceleration voltage is lowered (older ions have less internal energy) on the VG 70-70 instrument, i.e. the result approaches the result obtained on the JMS-HX110/HX110A instrument (where the ions have less internal energy). The same trend is observed when using the JMS-HX110/HX110A instrument. The results from both instruments seem to be at least qualitatively consistent with respect to the internal energy. This phenomenon is currently under study.

The proton affinity difference between CD_3–X–R and CH_3–X–R (X = O or NH, R = H or n-C_mH_{2m+1}) seem to be independent of X and R for the systems studied. Furthermore, ΔPA_{theo} and ΔPA_{exp} are seen to be qualitatively consistent.

The JMS-HX110/HX110A instrument is clearly more sensitive towards measuring kinetic isotope effects and effective temperatures. The following discussion will concentrate on results obtained on this instrument. The effective temperatures of the CD_3OH system (86 K) and the CD_3CN system (82 K) are approximately equal. Because these two systems have the same size (i.e. no size effect) it could be argued that under the given conditions metastable proton bound alcohol and nitrile homodimers (of the same size) will have the same effective temperature (i.e. contain the same amount of internal energy). The difference in bond strength between the CD_3OH system and the CD_3CN system is 2.7 kcal/mol [63], which apparently has no effect on the relative effective temperature (unless other factors have cancelled out the difference). The CD_3OCH_3 system is larger (~50% more degrees of freedom) and, presumably because of the size difference, have a higher effective temperature (212 K). The effective temperature for the $(CD_3)_2CO$ system (1502 K) has a large uncertainty (± 755 K), but even considering this it can be compared to the CD_3OCH_3 system, which is of similar size. This suggests that ketones have higher effective temperatures than amines, alcohols, ethers and nitriles (of similar size). The CD_3NH_2 system has a low effective temperature (44 K). The size of this system is comparable with the CD_3OH and CD_3CN system, suggesting that amines have lower effective temperatures compared to the other types of compounds of similar size that have been studied. Proton bound dimers of nitriles and oxygen bases have bonding energies in the range 27–33 kcal/mol. Proton bound amine dimers, in contrast have binding energies in the range 23–27 kcal/mol, depending on the size of the amine. It is therefore not surprising that the bond strength (the well depth, Fig. 6) is smaller for the CD_3NH_2 system (26.8 kcal/mol, Table 2) compared to the other systems, CD_3OH (32.3 kcal/mol), CD_3OCH_3 (30.3 kcal/mol), CD_3CN (29.6 kcal/mol) and $(CD_3)_2CO$ (30.0 kcal/mol) [63]. This could be a contributing factor for the low effective temperature observed for the CD_3NH_2 system.

Once again considering the results obtained on the JMS-HX110/HX110A instrument, the kinetic isotope effects, k_H/k_D, can be compared with the effect of labeling on the kinetic energy release, KER_H/KER_D (Fig. 10). As is evident from Fig. 10, KER_H/KER_D is observed to increase with increasing k_H/k_D. Fitting a straight line to the points results in a correlation coefficient of 0.985 (0.999 if CD_3CN is disregarded). This relationship can be rationalized from Fig. 6. As discussed earlier, the size of the kinetic isotope effect is dependent on the amount of internal energy (i.e. the value of the parameter called the effective temperature). For large E values (Fig. 6) or T_{eff} values the difference in the critical energies, $E_{0,D}$ and $E_{0,H}$ (Fig. 6), become less important, which in turn will result in smaller kinetic isotope effects. The same argument can be used for KER_H/ KER_D. For large internal energies the difference between KER_D and KER_H become less important, which in turn will result in a lower KER_H/KER_D ratio.

4. Conclusion

The dissociation reactions of isotope labeled proton bound dimers, (B)(B-d_n)H^+, have been studied with mass spectrometric methods, using high and low-pressure ionization. Proton transfer reactions between deuterium labeled amines, B-d_n, and unlabeled amines, B, have been studied with ab initio theory and using equilibrium methods.

Normal isotope effects were observed for all of the amine systems studied, consistent with the results from the theoretical study.

A small isotope effect on the enthalpy of association (~0.1 kcal/mol) and on the enthalpy of proton exchange (~0.2 kcal/mol) was observed. Because of the sensitivity of the experiment it was not possible to determine if the label position, size or structure of the proton bound dimer was important.

Kinetic isotope effects were measured from MIKES experiments for the dissociation reaction. The

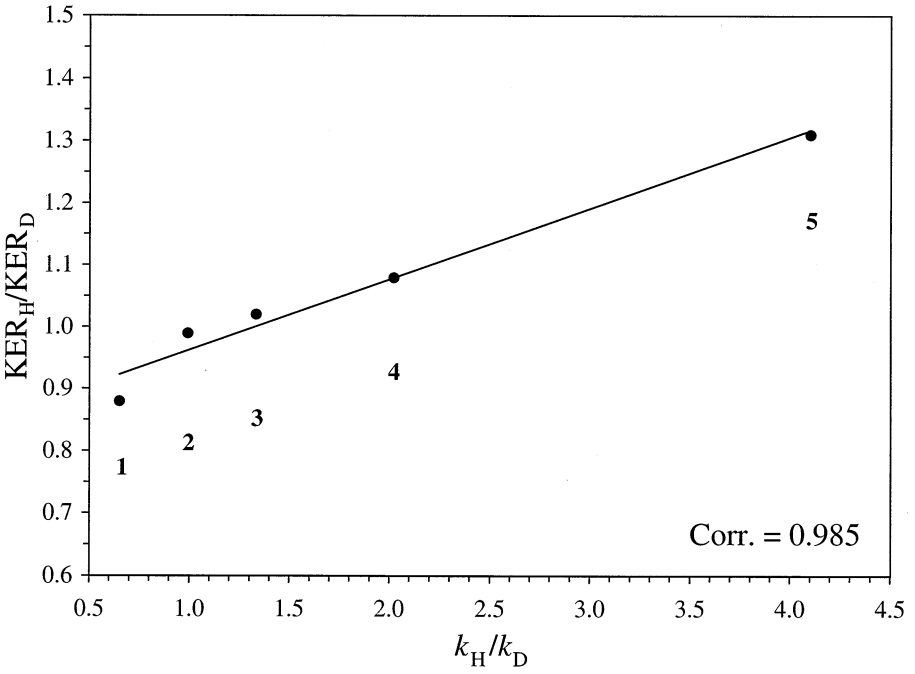

Fig. 10. Plot of KER_H/KER_D vs k_H/k_D (Eq. (9)) for proton bound dimers, (B)(B-d_n)H^+ (B = CH_3CN (**1**), $(CH_3)_2CO$ (**2**), CH_3OCH_3 (**3**), CH_3OH (**4**), CH_3NH_2 (**5**)) Instrument: JMS-HX110/HX110A.

kinetic isotope effects were measured at different ion lifetimes. Larger kinetic isotope effects were observed with lower internal energies. The magnitude of the isotope effects for the dissociation reactions was found to depend on the label position, size and structure of the proton bound dimer. The magnitude of the kinetic isotope effect was found to vary with the number and position of the deuterium label in the following way: α-$d_3 > \alpha$-$d_2 > \beta$-d_3. When high-pressure ionization was used, this order changed to: α-$d_3 > \beta$-$d_3 > \alpha$-d_2, inconsistent with observations discussed earlier. For larger systems smaller kinetic isotope effects were observed.

The extent of deuterium substitution were found to affect the observed isotope effect. The *n*th root (where *n* is the number of deuterium atoms) of the kinetic isotope effect will correct it to be per deuterium atom. This correction was applied and found to be suitable.

Effective temperatures have been calculated for all of the metastable proton bound amine dimers that were studied. The effective temperature is seen to follow the trend expected for the internal energy, which suggest that the effective temperature may be qualitatively consistent with the internal energy.

Excess energies for the metastable proton bound amine dimers were determined from measured kinetic isotope effects as well as from KER measurements. The two sets of results were found to differ by essentially a constant ratio, that is, the two sets of results were qualitatively consistent. This suggests that the use of the kinetic method, and the assumption that the effective temperature is described as the excess energy per mode in the metastable proton bound dimer, are supported.

Small effects of the deuterium labeling on the KER for the dissociation reactions were observed, when low-pressure ionization was employed, in favor of loss of the unlabeled amine ($KER_H/KER_D \approx 1.02$). Because of the subtlety of the effects it was not possible to determine if the label position, size or structure of the proton bound dimer was important.

Analogous nonsystematic studies of other com-

pound classes (CH_3OH, $(CH_3)_2O$, CH_3CN and $(CH_3)_2CO$) showed normal isotope effects, except for the proton bound dimer of CH_3CN and CD_3CN, which showed an inverse isotope effect. This system gives a normal kinetic isotope effect when high-pressure ionization is used, inconsistent with observations discussed earlier. Ab initio calculations revealed that protonation of CD_3CN will not be entropically favored at any temperature studied, which rules out an entropy effect to be the cause of the discrepancy when high pressure ionization is used. An expected direct proportionality between k_H/k_D and KER_H/KER_D was found for these systems.

Acknowledgements

T.B.M. acknowledges the Natural Sciences and Engineering Research Council of Canada for financial support. Dr. Steen Hammerum is gratefully acknowledged for helpful discussions. The authors thank Dr. Jan E. Szulejko for technical advice.

References

[1] P.J. Derrick, K.F. Donchi, in Comprehensive Chemical Kinetics, C.H. Bamford, C.F.H. Tipper (Eds.), Elsevier, Amsterdam, 1981, Vol. 24, pp. 53.
[2] P.J. Derrick, in Current Topics in Mass Spectrometry and Chemical Kinetics, J.H. Beynon, M.L. McGlashan (Eds.), Heyden, London, 1982, pp. 61.
[3] P.J. Derrick, Mass Spectrom. Rev. 2 (1983) 285.
[4] R.H. Shapiro, T.E. McEntee, D.L. Coffen, Tetrahedron. 24 (1968) 2809.
[5] F.W. McLafferty, D.J. McAdoo, J.S. Smith, R. Kornfeld, J. Am. Chem. Soc. 93 (1971) 3720.
[6] R. Neeter, N.M.M. Nibbering, Org. Mass Spectrom. 7 (1973) 1091.
[7] R.D. Smith, J.H. Futrell, Org. Mass Spectrom. 11 (1976).
[8] G. Eadon, R. Zawalski, Org. Mass Spectrom. 12 (1977) 599.
[9] G. Jones II, L.P. McDonnel-Bushnell, J. Org. Chem. 43 (1978) 2184.
[10] W.J. Broer, W.D. Weringa, Org. Mass Spectrom. 14 (1979) 36.
[11] D.J. DeFrees, M. Taagepera, B.A. Levi, S.K. Pollack, K.D. Summerhays, R.W. Taft, M. Wolfsberg, W.J. Hehre, J. Am. Chem. Soc. 101 (1979) 5532.
[12] M. Mruzek, G. Bouchoux. Int. J. Mass Spectrom. Ion Phys. 33 (1980) 301.
[13] G. Bouchoux, M. Mruzek, Adv. Mass Spectrom. 8 (1980) 90.
[14] S. Ingemann, S. Hammerum, Adv. Mass Spectrom. 8 (1980) 647.
[15] P.T. Mead, K.F. Donchi, J.C. Traeger, J.R. Christie, P.J. Derrick, J. Am. Chem. Soc. 102 (1980) 3364.
[16] K.F. Donchi, R.T.C. Brownlee, P.J. Derrick, J. Chem. Soc., Chem. Commun. (1980) 1061.
[17] T. Baer, R. Kary, Chem. Phys. Lett. 92 (1982) 659.
[18] W. Tumas, R.F. Foster, M.J. Pellerite, J.I. Brauman, J. Am. Chem. Soc. 105 (1983) 7464.
[19] S. Nascon, A.G. Harrison, Org. Mass Spectrom. 20 (1985) 429.
[20] W. Tumas, R.F. Foster, M.J. Pellerite, J.I. Brauman, J. Am. Chem. Soc. 109 (1987) 961.
[21] S. Ingemann, S. Hammerum, P.J. Derrick, J. Am. Chem. Soc. 110 (1988) 3869.
[22] S. Ingemann, S. Hammerum, P.J. Derrick, R.H. Fokkens, N.M.M. Nibbering, Org. Mass Spectrom. 24 (1989) 885.
[23] S. Ibrahim, C.I.F. Watt, J.M. Wilson, C. Moore, J. Chem. Soc., Chem. Commun. (1989) 161.
[24] S. Ingemann, E. Kluft, N.M.M. Nibbering, C.E. Allison, P.J. Derrick, S. Hammerum, Org. Mass Spectrom. 26 (1991) 875.
[25] B.D. Nourse, R.G. Cooks, Int. J. Mass Spectrom. Ion Processes 106 (1991) 249.
[26] M.J. Haas, A.G. Harrison, Int. J. Mass Spectrom. Ion Processes 124 (1993) 115.
[27] T.T. Dang, E.L. Motell, M.J. Travers, E.P. Clifford, G.B. Ellison, C.H. DePuy, V.M. Bierbaum, Int. J. Mass Spectrom. Ion Processes 123 (1993) 171.
[28] R.A.J. O'Hair, S. Gronert, T.D. Williams, Org. Mass Spectrom. 29 (1994) 151.
[29] P.J. Robinson, C.A. Holbrook, Unimolecular Reactions, Wiley, New York, 1972.
[30] W. Forst, Theory of Unimolecular Reactions, Academic, New York, 1973.
[31] R.G. Cooks, J.H. Beynon, R.M. Caprioli, G.R. Lester, Metastable Ions, Elsevier, Amsterdam, 1973.
[32] R.G. Cooks, T.L. Kruger, J. Am. Chem. Soc. 99 (1977) 1279.
[33] S.A. McLuckey, D. Cameron, R.G. Cooks, J. Am. Chem. Soc. 103 (1981) 1313.
[34] R.G. Cooks, J.S. Patrick, T. Kotiaho, S.A. McLuckey, Mass Spectrom. Rev. 13 (1994) 287.
[35] K. Vékey, J. Mass Spectrom. 31 (1996) 445.
[36] S.G. Lias, J.E. Bartmess, J.F. Liebman, J.L. Holmes, R.D. Levin, W.G. Mallard, J. Phys. Chem. Ref. Data, Suppl. 1 (1988).
[37] J.J. Grabowski, C.H. DePuy, J.M. van Doren, V.M. Bierbaum, J. Am. Chem. Soc. 107 (1985) 7384.
[38] D.J. DeFrees, J.E. Bartmess, J.K. Kim, R.T. McIver Jr., W.J. Hehre, J. Am. Chem. Soc. 99 (1977) 6451.
[39] S.E. Barlow, T.T. Dang, V.M. Bierbaum, J. Am. Chem. Soc. 112 (1990) 6832.
[40] G. Boand, R. Houriet, T. Gaumann, J. Am. Chem. Soc. 105 (1983) 2203.
[41] R.W. Taft, in Proton Transfer Reactions, E.F. Caldin, V. Gold (Eds.), Wiley, New York, 1975, pp. 31.
[42] J.E. Szulejko, T.B. McMahon, Int. J. Mass Spectrom. Ion Processes 109 (1991) 279.
[43] M.J. Frisch, G.W. Trucks, H.B. Schlegel, P.M.W. Gill, B.G.

Johnson, M.A. Robb, J.R. Cheeseman, T. Keith, G.A. Petersson, J.A. Montgomery, K. Raghavachari, M.A. Al-Laham, V.G. Zakrzewski, J.V. Ortiz, J.B. Foresman, C.Y. Peng, P.Y. Ayala, W. Chen, M.W. Wong, J.L. Andres, E.S. Replogle, R. Gomperts, R.L. Martin, D.J. Fox, J.S. Binkley, D.J. Defrees, J. Baker, J.P. Stewart, M. Head-Gordon, C. Gonzalez, J.A. Pople, GAUSSIAN94, Revision B.3, Gaussian, Inc., Pittsburgh, PA, 1995.
[44] A.P. Scott, L. Radom, J. Phys. Chem. 100 (1996) 16 502.
[45] S.A. Shaffer, F. Turecek, J. Am. Chem. Soc. 115 (1993) 12 117.
[46] L.R. Hall, R.T. Iwamoto, R.P. Hanzlik, J. Org. Chem. 54 (1989) 2446.
[47] R.G. Kostyanovsky, V.G. Plekhanov, Org. Mass Spectrom. 6 (1972) 1183.
[48] M.J. Raftery, J.H. Bowie, Aust. J. Chem. 41 (1988) 1477.
[49] P.J. Krueger, J. Jan, Can. J. Chem. 48 (1970) 3229.
[50] K.B. Tomer, Org. Mass Spectrom. 10 (1975) 480.
[51] J.L. Holmes, J.K. Terlouw, Can. J. Chem. 54 (1976) 1007.
[52] C.H. Bushweller, S.H. Fleischman, G.L. Grady, P. McGoff, C.D. Rithner, M.R. Whalon, J.G. Brennan, R.P. Marcantonio, R.P. Domingue, J. Am. Chem. Soc. 104 (1982) 6224.
[53] T. Bjørnholm, S. Hammerum, D. Kuck, J. Am. Chem. Soc. 110 (1988) 3862.
[54] R.D. Bowen, A.G. Harrison, Org. Mass Spectrom. 16 (1981) 180.
[55] R.D. Bowen, D.H. Williams, G. Hvistendahl, J. Am. Chem. Soc. 99 (1977) 7509.
[56] J. Zavada, M. Svoboda, J. Sicher, Collect. Czech. Chem. Commun. 33 (1968) 4027.
[57] R.N. Renaud, L.C. Leitch, Can. J. Chem. 46 (1968) 385.
[58] J. Tanaka, J.E. Dunning, J.C. Carter, J. Org. Chem. 31 (1966) 3431.
[59] T.D. Goldfarb, B.N. Khare, J. Chem. Phys. 46 (1967) 3379.
[60] R. Williamson, in Methoden der Organischen Chemie (Houben-Weyl), Eugen Müller (Ed.), Georg Thieme Verlag, Stuttgart, 1965, Vol. 613, pp. 26.
[61] S.L. Craig, M. Zhong, B. Choo, J.I. Brauman, J. Phys. Chem. A 101 (1997) 19.
[62] K.H. Lund, G. Bojesen, Int. J. Mass Spectrom. Ion Processes 156 (1996) 203.
[63] Measured by Dr. J.E. Szulejko, University of Waterloo, unpublished results.